PROGRESS REPORT

PROJECT TITLE: Sustainable polyesters from corn as tomorrow's advanced plastics
PROJECT NUMBER: 1094-19EU
REPORTING PERIOD: 1 April 2019 – 30 June 2019
PRINCIPAL INVESTIGATOR: Marc A. Hillmyer
ORGANIZATION: University of Minnesota
PHONE NUMBER: 612.625.7834
EMAIL: hillmyer@umn.edu

1.) PROJECT ACTIVITIES COMPLETED DURING THE REPORTING PERIOD. (*Describe project progress specific to goals, objectives, and deliverables identified in the project workplan.*)

Mechanically tough and transparent melt blown PLA film: The Bates and Ellison groups have previously shown the ability to toughen poly(lactide) (PLA) with diblock copolymers. Specifically, we have used a commercially available) diblock copolymer poly(ethylene oxide)-b-poly(butylene oxide) (PEO-PBO) (trade name Fortegra™ 100 from Olin Corporation) as an additive. When blended with PLA, the PEO-PBO diblock copolymer can both toughen PLA and prevent the aging of PLA by forming spherical domains. To continue investigating the toughening mechanics of PEO-PBO in PLA, new PEO-PBO was recently purchased from Olin Corporation. But, the newly acquired PEO-PBO has different chemical characteristics than the previously received PEO-PBO and showed inconsistent toughening in PLA. This report summarizes the differences in PLA blend performance using the previously acquired PEO-PBO diblock copolymer, referred to "old" PEO-PBO-o, and the recently purchased product referred to as "new" PEO-PBO-n.

Biobased PLA nanocomposites using cellulose nanocrystals: Film blowing, also referred to as blown film extrusion,[1-2] is a commercial processing technique that produces ~160 million metric tons[3-4] of polymer films for flexible packaging annually. Non-renewable, petroleum-based polymers, such as polyethylene, polypropylene, and poly(ethylene terephthalate), have dominated the film blowing industry.[5] The successful implementation of corn-derived and bio-degradable poly(lactide) (PLA) in the film blowing process will greatly advance the use of sustainable materials for replacing traditional petroleum-based polymers. This project is focused on film blowing PLA that is toughened with diblock copolymers (BCPs), i.e., commercial poly(ethylene oxide)-b-poly(butylene oxide) (PEO-PBO) called Fortegra™ by Olin Corporation, and cellulose nanocrystal (CNC) additives. Film blowing of BCP/PLA blends builds on a complementary project that is focused on "BCP additives development for PLA" led by Frank Bates and Christopher Ellison, while film blowing of CNC/PLA blends relies on the development of CNC additives as

appropriate toughening agents for PLA. This report summarizes the film blowing of both neat PLA and Fortegra/PLA blends as well as the synthesis of CNCs (in collaboration with Prof. Stuart Rowan at University of Chicago).

Polyesters from 3-hydroxypropionic acid: The Hillmyer group worked on the synthesis of sustainable telechelic polyesters in order to access complex and degradable polymer architectures (*e.g.*, thermoplastic elastomers). Polymers of molar masses <5,000 g.mol^{-1} were targeted in order to have a clear chain-end characterization. The strategy is to use a hydroxy cyclic ketone as an initiator for the polymerization. The second part is to oxidize the ketone chain-end to obtain a lactone as chain-end. Conditions were optimized in order to do these steps in a one-pot process. Polymers were analyzed by ^{1}H and ^{13}C NMR, MALDI-TOF as well as chloroform SEC. The second part of the project was the study of graft-through polymerization of those telechelic polyesters with lactones.

Biobased terephthalic acid from corn-derived products: In Q1, the Dauenhauer group has completed the initial design of a chemical process to manufacture butadiene from corn-derived sugars. The specific goal was to combine chemical reactors and separators into a system that could utilize sugar-derived furfural and convert that into butadiene with the purity specifications required for commercial-grade rubber and plastic. Specific objectives included: (1) identifying optimal reactor conditions, (2) selecting separator recycle conditions, (3) identifying the needs for solvents. The concept of the process is described in the figure below.

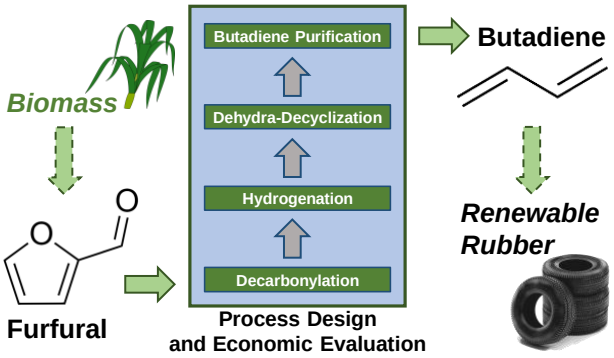

Figure 1

2.) IDENTIFY ANY SIGNIFICANT FINDINGS AND RESULTS OF THE PROJECT TO DATE.

Mechanically tough and transparent melt blown PLA film

The molecular weights and dispersity of each PEO-PBO diblock copolymer were determined by size exclusion chromatography-multi angle light scattering (SEC-MALS) with dimethylformamide (DMF) containing 0.05M of lithium bromide (LiBr) as the mobile phase (Figure 2). Based on the SEC traces in Figure 1, it is evident that PEO-PBO-n diblock copolymer is larger in molecular weight than PEO-PBO-o. Using a dn/dc value of 0.0298, the molecular weight of the new and old PEO-PBO are 7.4 kg/mol and 4.3 kg/mol, respectively. This difference in molecular weights can affect the dispersion of PEO-PBO in PLA. PEO-PBO-o and

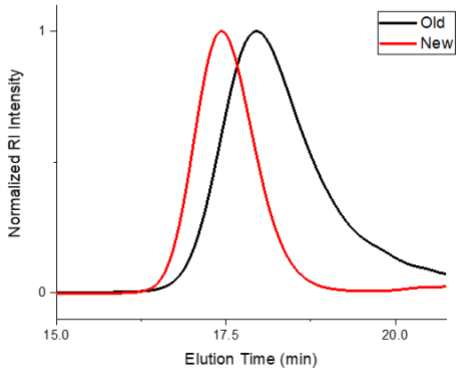

Figure 2. SEC traces of the two different PEO-PBO diblock copolymers run in DMF containing 0.05M of LiBr as the mobile phase at a flowrate of 1mL/min.

PEO-PBO-n have 33% and 39% by mass PEO respectively, as determined by ^{1}H NMR.

A blend of PEO-PBO-n in PLA was prepared by the same masterbatch approach summarized in previous reports. The masterbatch was made up of 25 % wt. PEO-PBO and 75 % wt. PLA (NatureWorks 4060D). The masterbatch and additional PLA were fed into a micro compounder at 180°C resulting in a 5 % wt. PEO-PBO in PLA blend. To characterize the blend, differential scanning calorimetry (DSC), scanning electron microscopy (SEM) and tensile tests were performed on the blends as described below.

Tensile tests were performed to investigate the effect of the diblock copolymers on the toughenes of PLA. The tensile tests were undertaken on a Shimadzu Autograph AGS-X Tensile Tester at room temperature with an extension rate of 10 mm/min following ASTM D1708. Figure 3A shows tensile tests performed on the PEO-PBO-o/PLA blend at different aging times. As described in previous reports, the mechanical properties are consistently tough and remarkably independent of aging time. Figure 3B displays tensile tests obtained with the PEO-PBO-n/PLA blend; all samples were aged for the same amount of time, 48 hrs. Surprisingly, the elongation at break varies greatly between repeated tensile experiments. Most samples break before 35% strain, while a few reach values greater than 150%. This inconsistency in mechanical properties is detrimental for applications.

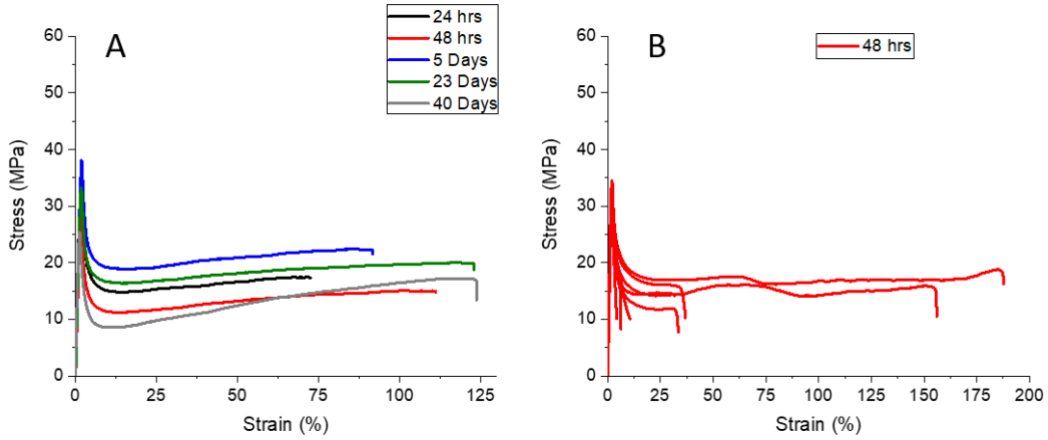

Figure 3. (A) Tensile results for 5% wt. PEO-PBO-o in PLA tested at different aging times. (B) Tensile results for 5% wt. PEO-PBO-n at 48 hrs. All tests were run at a cross head speed of 10 mm/min at room temperature.

To investigate potential reasons for the differences in mechanical properties, SEM was employed to examine the morphology of the PEO-PBO/PLA blends. The samples were prepared by microtoming at −120°C to create a fresh cross section and then the samples were placed in ethanol to dissolve the PEO-PBO diblock copolymer. The resulting cross sections were sputter coated with 2nm of iridium and imaged with a JEOL 6500 SEM. Figure 4 shows representative SEM images and corresponding size distribution of the particle diameters for PEO-PBO-o/PLA blend (Figure 4A-B) and PEO-PBO-n/PLA blend (Figure 4C-D). The dispersion sizes are different, which may be due to the difference in molecular weight. The PEO-PBO-n dispersion size has an average particle diameter of 0.87±0.52μm, compared to the PEO-PBO-o blend dispersion size of 0.66±0.35

µm. Although the average particle sizes are relatively similar, the blends exhibit much different mechanical properties. This is not expected and will be the focus of our future work.

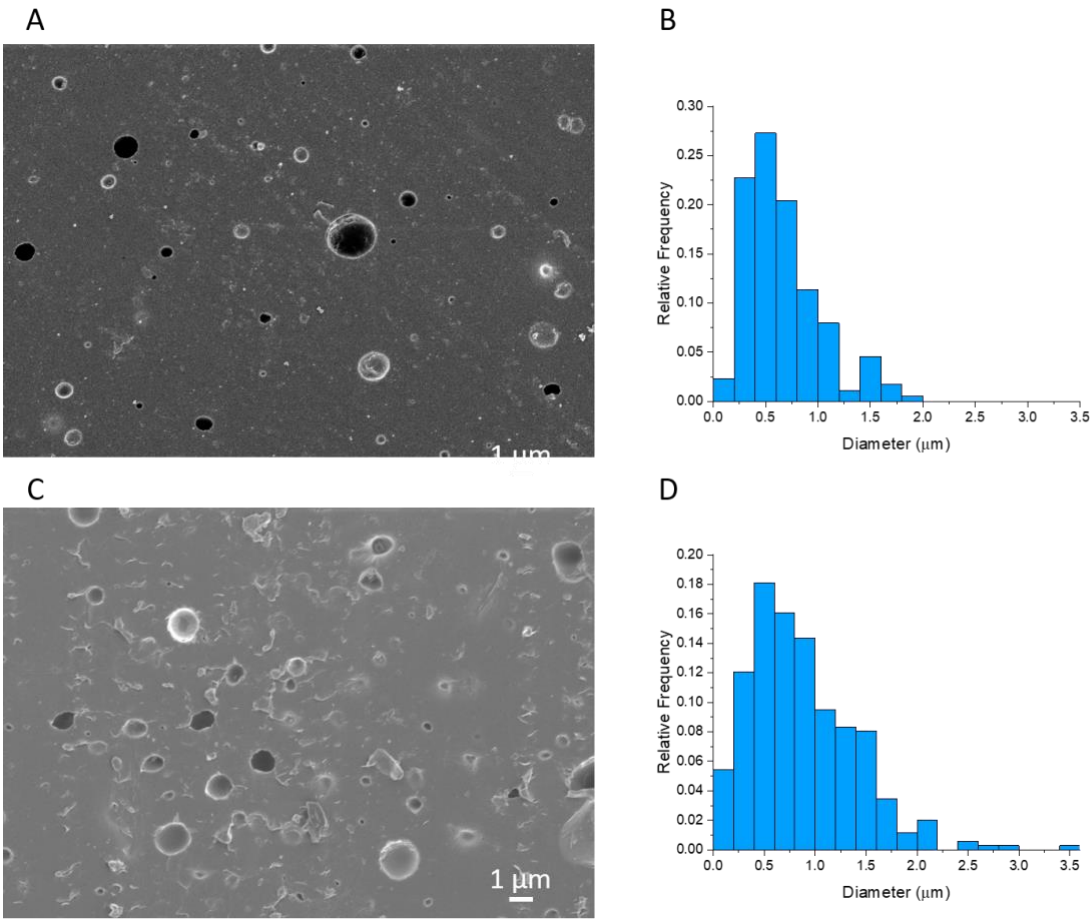

Figure 4. (A) SEM image of 5% wt. PEO-PBO-o in PLA, after washing the microtomed surface with ethanol to dissolve the PEO-PBO diblock copolymer. (B) Relative frequency histogram of particle diameters of 5% wt. PEO-PBO-o in PLA. (C) SEM image of 5% wt. PEO-PBO-n in PLA, after washing the microtomed surface with ethanol to dissolve the PEO-PBO diblock copolymer. (D) Relative frequency histogram of particle diameters of 5% wt. PEO-PBO-n in PLA.

To explore how differences in molecular weight, and composition, result in differences in mechanical properties, we synthesized additional PEO-PBO diblock copolymers by a two-step anionic polymerization. First, poly(butylene oxide) was synthesized with a terminal hydroxyl group followed by reinitiation and addition of ethylene oxide using a modified version of the method reported by Allgaier et al.[5] Butylene oxide was pre-dried over calcium hydride overnight, followed by distillation from butyl magnesium chloride twice. Tetrahydrofuran (THF) was collected from an alumina column as described elsewhere.[6] The polymerization initiator, potassium tert-butoxide, was injected into the solvent in the reactor under 3 psi argon pressure. Crown ether, that was dissolved in benzene and freeze dried, was then added to the reactor. Crown ether complexes with the potassium counter ion, leading to narrow dispersities and higher

molecular weights while limiting the side reactions. The purified butylene oxide was then added and allowed to react for 48 hours at room temperature. The polymer solution was rotary evaporated then dissolved in hexanes and washed with water twice to remove the crown ether and potassium salts. The polymer was vacuum dried before the addition of the second block. Ethylene oxide was twice purified by reaction with butyl magnesium chloride. PBO is dissolved in purified THF and initiated by titrating with potassium naphthalenide followed by the addition of EO and allowed to react overnight at 40°C. The reaction was terminated by the addition of degassed methanol. The final polymer solution is rotary evaporated, filtered, and vacuum dried to purify the polymer. SEC traces of the PBO and associated PEO-PBO diblock copolymer that was synthesized with a molecular weight of 4.0 kg/mol and containing 31% by mass PEO are shown in Figure 5. The individual symmetric SEC traces evidence a successful polymerization. These PBO-PEO diblock copolymers will be blended with the commercial PLA and evaluated by SEM and tensile testing.

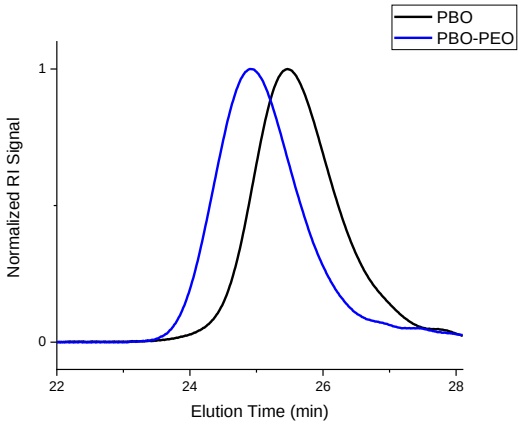

Figure 5. SEC traces of the two-step anionic polymerization of PEO-PBO, with THF as the mobile phase.

Biobased PLA nanocomposites using cellulose nanocrystals

Film blowing of neat PLA and Fortegra/PLA blends: A masterbatch of 9/91 wt% Fortegra/PLA (amorphous PLA, NatureWorks 4060D) blend was prepared by melt mixing predetermined amounts of Fortegra and PLA in a twin-screw extruder operated at 180 °C and 60 RPM. The Fortegra™ 100 used here is a PEO-PBO diblock copolymer with a total molecular weight of 7400 g/mol (by SEC-MALS) and 33 wt% PEO (by 1H NMR); see the complementary project report from Frank Bates and Christopher Ellison for detailed characterization. The Fortegra content in the masterbatch was confirmed to be 9 wt% by gravimetric analysis before and after solvent (i.e., methanol) extraction of Fortegra from the PLA matrix.

Predetermined amounts of the masterbatch and neat PLA were physically mixed at room temperature and then fed into the extruder, resulting in Fortegra/PLA samples containing 0, 1 and 5 wt% Fortegra. Film blowing of both neat PLA and Fortegra/PLA blends (at 1 and 5 wt% Fortegra) was successfully conducted on a lab-scale blown film extrusion line (Figure 6, left) equipped with a single screw extruder at the University of Minnesota. In a typical film blowing process (Figure 6, middle), a polymer melt is extruded through an annular film die, and then the extrudate is drawn as a bubble that expands radially because of the internal pressure applied by the central air inlet while axial tension is imposed by the rotation of the nip rolls; the nip rolls also form an air-tight seal to maintain the film bubble internal pressure.[2] Detailed film processing parameters include: extruder temperature of 200 °C; screw rotation speed at 200 rpm; tubular film die diameter of 25 mm inner diameter and 28 mm outer diameter; nip rolls drawing speed at 6.0 ft/min. Film blowing of both neat PLA and Fortegra/PLA blends resulted in thin, transparent films with diameters ranging from 3 – 5 cm and thicknesses ranging from 30 – 100 μm. A representative neat PLA blown film is shown in Figure 6, right.

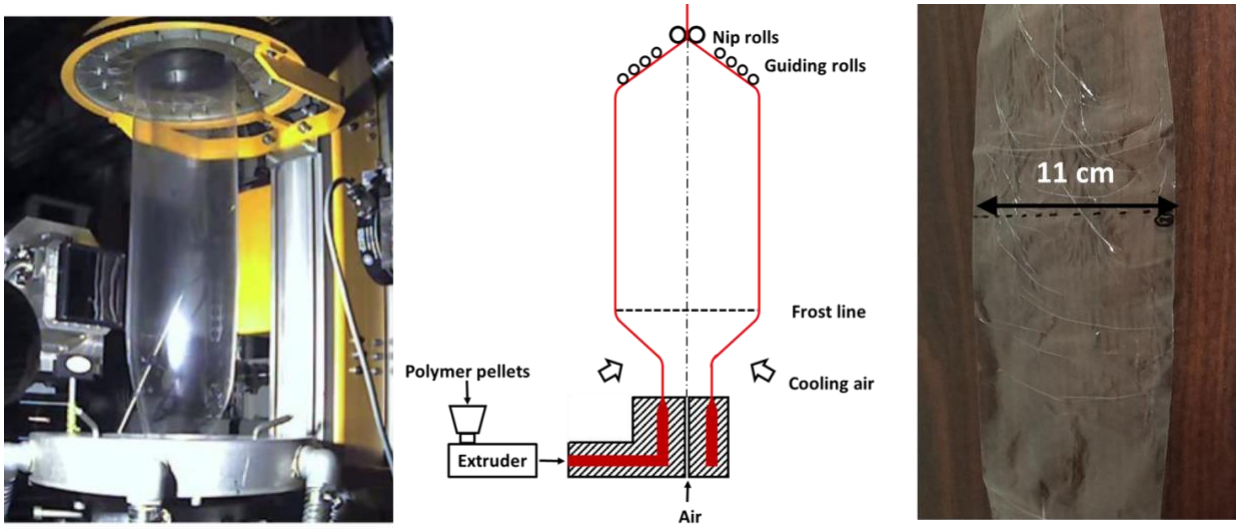

Figure 6. (Left) A photograph of the lab-scale film blowing line at the University of Minnesota and (middle) schematic of the film blowing process. (right) A representative neat PLA film obtained from this process

Morphology of Fortegra/PLA blends before and after film blowing: The Fortegra/PLA blend morphologies before and after film blowing were examined by scanning electron microscopy (SEM; Hitachi S-4700). The samples (i.e., 9/91 wt% Fortegra/PLA bulk pellets and Fortegra/PLA blown films) were freeze-fractured in liquid nitrogen, followed by rinsing the fresh cross-section with methanol to remove Fortegra. The resulting cross-sections were sputter coated with about 5 nm of iridium (ACE600 Coater) for morphological characterization by SEM. Figure 7A shows a representative SEM image of the resulting cross-section of the 9/91 wt% Fortegra/PLA bulk pellet. The nearly spherical ~0.5 to ~2.5 µm diameter cavities in Figure 7A correspond to the removed Fortegra phase. Figure 7B shows a representative SEM image of the resulting cross-section of the 5/95 wt% Fortegra/PLA blown film. Similarly, the elongated, ellipsoidal cavities in Figure 7B correspond to the removed Fortegra phase, whose diameters range from ~0.2 to ~0.5 µm near their widest point. Both Figure 7A and 7B indicate Fortegra is thermodynamically incompatible with PLA and dispersed as a minor phase within the PLA matrix, regardless of sample geometry (i.e.,

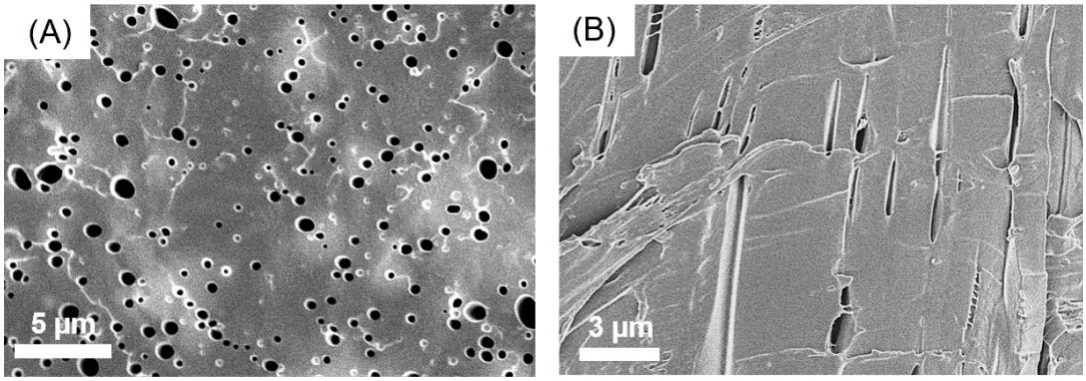

Figure 7. Representative SEM images after Fortegra removal from cross-sections of (A) 9/91 wt% Fortegra/PLA bulk pellets and (B) 5/95 wt% Fortegra/PLA blown films.

bulk pellet vs film). More detailed analysis of the Fortegra dispersion is currently being performed to examine the effects of film blowing on the blend morphology.

Thermal properties of neat PLA and Fortegra/PLA blends: Thermal properties of both neat PLA and Fortegra/PLA blends were characterized using a Mettler Toledo DSC 1 differential scanning calorimetry (DSC) instrument. All the samples were first annealed at 150 °C for 15 min to erase thermal history and then quenched to -100 °C at 20 °C/min. These samples were then heated to 150 °C at 10 °C/min, and the corresponding DSC thermograms are shown in Figure 8. The neat PLA showed a glass transition temperature (T_g) at 56°C, while the neat Fortegra exhibited a T_g of about -5 °C and a melting temperature (T_m) of ~8 °C. The 9/91 wt% Fortegra/PLA masterbatch pellets exhibited both a T_g and T_m for Fortegra as well as a T_g for PLA, which confirms the thermodynamic incompatibility between PLA and Fortegra consistent wih the morphology characterizations above. Interestingly, the Fortegra/PLA film samples did not exhibit thermal transitions representative of those of neat Fortegra as the 9/91 wt% Fortegra/PLA masterbatch pellets displayed. We hypothesize that film processing may have significant influence on the thermophysical properties of the Fortegra/PLA blends which is a well-known means by which film properties are tailored for applications. Additional research is needed to understand the details of these differences.

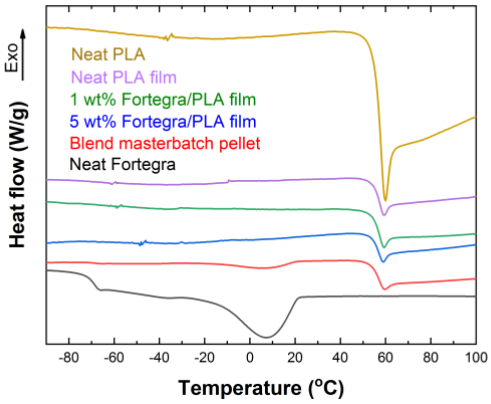

Figure 8. DSC thermograms taken on second heat for neat PLA, neat Fortegra, blend pellet from the Fortegra/PLA 9/91 wt% masterbatch and the Fortegra/PLA blend blown films with various Fortegra loadings (0, 1 and 5 wt%). The data are shifted vertically for clarity.

Blown film tensile properties: neat PLA and Fortegra/PLA blends: The tensile properties of both neat PLA and Fortegra/PLA blends as blown film were characterized. Tensile bar specimens were prepared according to ASTM D1708 by cutting the tensile bar with the long-axis in the extrusion direction of the blown film. All the samples were aged at room temperature for 24 hours before characterization. Tensile tests were conducted on a Shimadzu Autograph AGS-X Tensile Tester at room temperature with an extension rate of 10 mm/min following ASTM D1708. Figure 9 shows representative stress-strain data of the neat PLA and Fortegra/PLA (at 1 and 5 wt% Fortegra) blown films, and Table 1 compiles the tensile property values. According to Table 1, Young's modulus and ultimate strength for the Fortegra/PLA blend films were

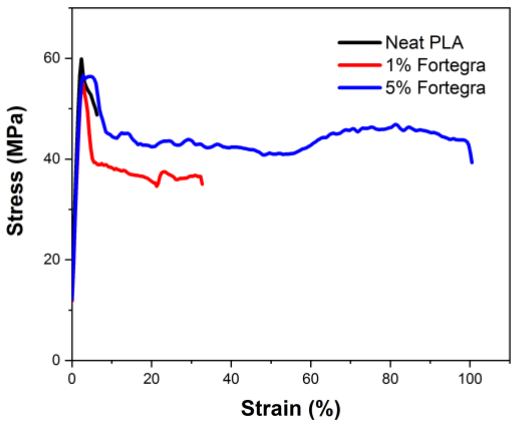

Figure 9. Representative stress-strain data for neat PLA and Fortegra/PLA (at 1 and 5 wt% Fortegra) blown films.

the same within error as the neat PLA films. Elongation at break increased from 6 (±3)% for neat PLA films to 123 (±68)% for 5 wt% Fortegra/PLA blend films. As a result, the toughness (defined as the total area under the stress-strain data) exhibited a ~20 fold increase from 2.8 (±1.2) MJ-m^{-3} for neat PLA films to 51 (±33) MJ-m^{-3} for 5wt% Fortegra/PLA blend films. The observed toughening effect is consistent with the previous reports for a complementary project focused on "BCP additives development for PLA" led by Frank Bates and Christopher Ellison. The next step is to examine the mechanical properties of blown films in different sampling directions as a function of aging time at room temperature. Additional research will also be focused on understanding the detailed toughening mechanism for blown film and the influence of processing conditions on thermophysical and microstructural properties.

wt % of Fortegra in Fortegra/PLA	Young's Modulus (GPa)	Ultimate Strength (MPa)	Elongation at Break (%)	Toughness (MJ m^{-3})
0	2.5 (±0.1)	61 (±1)	6 (±3)	2.8 (±1.2)
1	1.9 (±0.7)	54 (±18)	50 (±23)	26 (±22)
5	2.0 (±0.4)	53 (±10)	123 (±68)	51 (±33)

Table 1. Tensile properties of both neat PLA and Fortegra/PLA blend films. Average property values and standard deviations in parentheses are from five separate measurements.

Development of CNCs as toughening agents for PLA: Cellulose nanocrystals (CNCs) are rod-like in shape (typically 200 - 300 nm in length and ~10 nm in diameter) with high aspect ratio, large surface area, transparency, high strength and stiffness, and biodegradability, holding promise for use as reinforcing fillers in high-performance nanocomposites.[6-7] CNCs are typically obtained by isolating the crystalline domains from the purified cellulose (obtained from various bio-sources, e.g., lignocellulosic fibers) via acid hydrolysis.[8-9] This study is focused on developing CNC-based additives for toughening PLA, followed by film blowing of the toughened CNC/PLA polymer nanocomposites. To toughen PLA, CNC fillers need to be chemically decorated with rubbery polymers to activate toughening mechanisms such as cavitation, crazing and matrix shear yielding. Additional chain-end functionalization, either with a specific functional group or another polymer chain that is chemically compatible with PLA, is also needed to aid in CNC dispersion in the PLA matrix.

In the past quarter, both pristine and oxidized CNCs were successfully synthesized by our collaborators in Prof. Rowan's group at the University of Chicago. Pristine CNCs were isolated from natural miscanthus giganteus (MxG) stalks by removing the amorphous domain from the MxG via acid hydrolysis using hydrochloric acid (1 M).[8] The average diameter and length of the resulting pristine CNCs were characterized by transmission scanning electron microscopy to be 4.3 ± 0.9 nm and 298 ± 34 nm, respectively, resulting in an aspect ratio (defined as length/diameter) of ~70. The amount of C6 primary hydroxyls exposed on the microfibril surfaces was calculated to be ~1600 mmol/kg using crystal sizes of the original native cellulose and the CNC dimensions.[10] The primary hydroxyls on the surface of pristine CNCs (noted as CNC-OH) can be converted to carboxylate (-COOH) groups by TEMPO-oxidization following the same procedure used in a previous study,[8] resulting in oxidized CNCs (noted as CNC-COOH). CNC-COOH exhibited within error the same average diameter and length as those of CNC-OH, consistent with a previous observation that TEMPO-oxidation did not alter the overall CNC filler morphology.[11] The contents

of carboxylate groups on the surface of the resulting CNC-COOH fillers were measured to be ~1100 mmol/kg by titration.[8]

The next step is to functionalize the surfaces of both CNC-OH and CNC-COOH with rubbery polymers. For CNC-OH, ring opening polymerization (ROP) of ε-caprolactone and δ-valerolactone initiated by the hydroxyls on the CNC surface will be conducted to form CNCs grafted with rubbery polycaprolatone/polyvalerolactone chains. For CNC-COOH, carboxylate groups will be first converted to bromide groups, followed by surface-initiated atomic transfer radical polymerization (ATRP) of n-butyl acrylate (nBA) to render CNCs grafted with rubbery PnBA chains. Additional chain-end functionalization will be performed to aid dispersion of CNCs in the PLA matrix, if needed.

Polyesters from 3-hydroxypropionic acid

A three-step one-pot synthesis for chain-end functionalized PLLA was developed (Figure 10) in the Hillmyer group. Starting from 4-hydroxycyclohexanone (a cyclic ketone) as the initiator, L-Lactide was polymerized in bulk using an organocatalyst (1,8-Diazabicyclo[5.4.0]undec-7-ene, DBU). After 20 minutes, polymerization was stopped with acetic acid and the hydroxyl end group was acetylated using acetic anhydride. Different catalysts, reagents, temperatures and solvents were tested. Doing the acetylation without solvent, catalysts nor reagent at 100°C were found to give the best results: complete acetylation was obtained after 13 hours. Samples were analyzed after each step by ^{1}H NMR, chloroform SEC and MALD-TOF. Without purification, the ketone chain-end was then oxidized using 3-chloroperbenzoic acid (mCPBA). Different solvent and temperature were tested. After one hour at 40°C in ethyl acetate, complete conversion was obtained. The purified sample was analyzed by ^{1}H NMR, SEC and MALDI-TOF. This one-pot strategy allows us to have a facile, efficient and eco-friendly way to synthesize our new PLLA macromonomer.

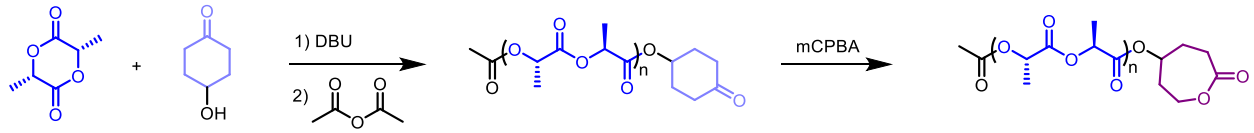

Figure 10. Lactone chain-end PLLA synthesis

We are studying the application of this strategy to γ-methyl-ε-caprolactone (γMCL) polymerization.

The graft-through polymerization of the synthesized telechelic PLLA with γMCL was studied (Figure 11). An experiment in C_6D_6 in an NMR tube showed the random character of the copolymerization. The conditions are optimized to obtain a controlled polymerization. Graft polymers different in length, MCL/LA ratio and grafting density will synthesized in order to measure their thermal and physical properties.

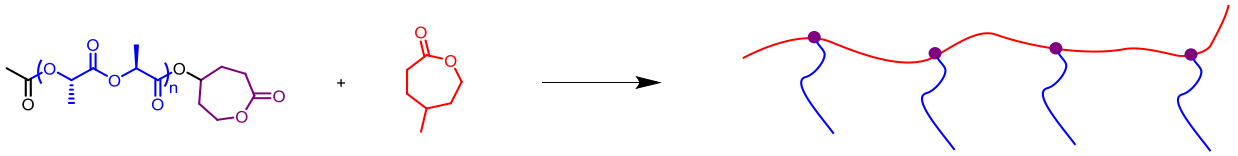

Figure 11. Graft-through polymerization

Development of hydroesterification as a new route to sustainable polymers

Since our previous funding cycle, the Tonks group has carried out initial hydroesterificative polymerization attempts of coumaric acid-derived monomers. However, these have shown radical styrene polymerization as a counterproductive side reaction, similar to what was observed in our initial VBA polymerization work. When BHT, a radical inhibitor, is used to prevent this side polymerization some ester formation is seen; however, the conversion of the reaction is low. The next step in this project is to determine what factors are hindering the formation of polyester products.

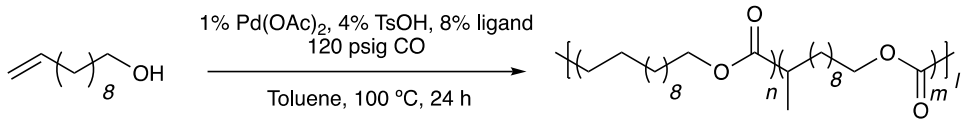

Figure 12: Hydroesterification of 10-undecenol

In our previous work we found that 10-undecenol, derived from seed oils, would effectively undergo hydroesterificative polymerization, resulting in polymers with molecular weights of 14.5 kg/mol after 16 hours. These polymers tend to form in a mixture of branched and linear products, as shown in Figure 12.

Currently, we are examining the role that the catalyst and ligand plays in the creation of branched and linear polymers. By tuning the branching of the polymer, the physical polymer properties will change, leading to polyesters with different potential uses. A variety of monophosphine ligands will be synthesized and tested for their effect on the hydroesterificative polymerization. An initial phosphine ligand has been made through the synthetic pathway shown in Figure 13. We suspect this ligand will lead to a product with higher branching density, based on similar reports in the literature for small-molecule hydroesterification. A key feature of the branched selectivity of this new ligand appears to be the *ortho* methoxy (OMe) group, although in our hands these *ortho* methoxy-derived ligands are so far less reactive than PPh_3. Synthesis of additional ligands will clarify why triphenylphosphine has performed best so far in this system.

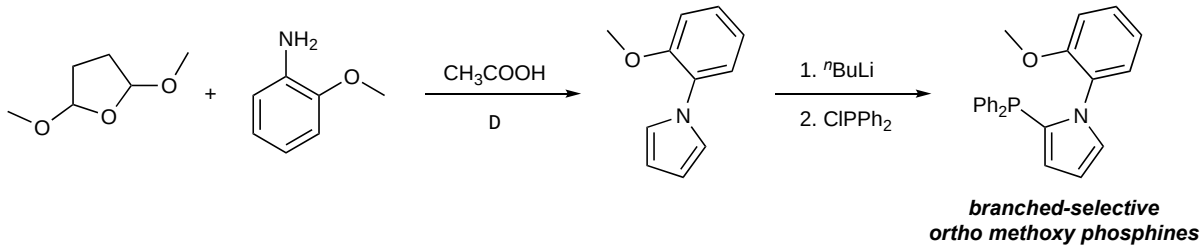

Figure 13: Synthesis of phosphine ligand featuring a pyrrole moiety

New polyester structures from corn-derived carboxylic acids

Hoye group researchers have extended their studies of the polymerization of 4-ketovalerolactone (**KVL**, Figure 14), a monomer available from levulinic acid. Specifically, they have explored the syntheses of a series of ABA triblock copolymers using, initially, valerolactone as the soft (midblock) segment and **KVL** as the precursor to the hard end blocks. ABA triblock polymers of

this architecture, namely a soft or rubbery center block (B) and two terminal blocks (A) of a hard (or more crystalline) nature represent a major subset of materials known as thermoplastic elastomers. Perhaps the most commonly known example is Kraton™. These thermally processable materials find myriad applications from shoe soles to 3D printing and beyond.

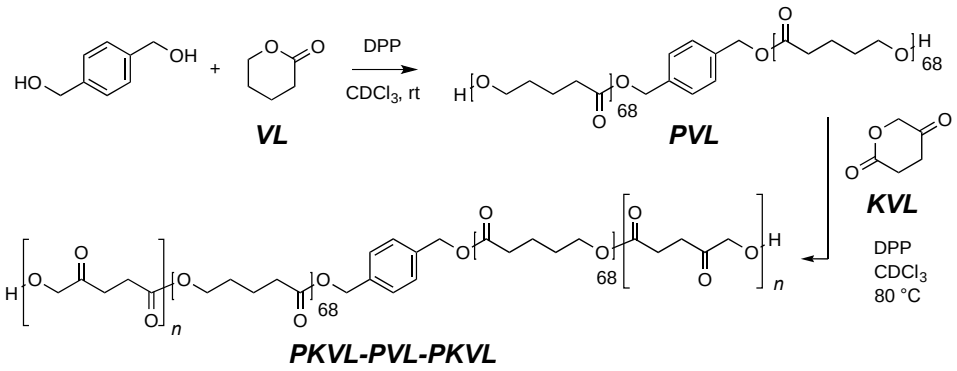

Figure 14. Preparation of **PKVL-PVL-PKVL** triblock copolymers.

The preparation of one of these novel **KVL**-based triblock copolymers is outlined in Figure 14. The initial midblock was prepared by initiating the polymerization of valerolactone (**VL**) with the difunctional initiator benzene-1,4-dimethanol. This poly(valerolactone) diol (**PVL**) was then treated with **KVL** to prepare the first samples of KVL-containing ABA polyesters.

VL:KVL	monomer conv.	yield	M_n (NMR)	M_n (SEC)	M_w (SEC)	$Đ$
100:0	95%	92%	13.6 k	15.0 k	20.0 k	1.33
80:20	60%	72%	18.9 k	20.0 k	26.3 k	1.32
90:10	85%	75%	18.7 k	18.0 k	25.4 k	1.41

Table 2. Characteristics of the synthetic **PKVL-PVL-PKVL** triblock copolymers.

A representative differential scanning calorimetry (DSC) thermogram of one of these triblock copolymers is shown in Figure 15. It shows a melting phase transition for the **PVL** moiety but, somewhat surprisingly, no significant glass transition nor melting characteristics for the **PKVL**. In light of this, the researchers next plan to replace **VL** with 4-methylcaprolactone to create a soft (amorphous) mid-block segment.

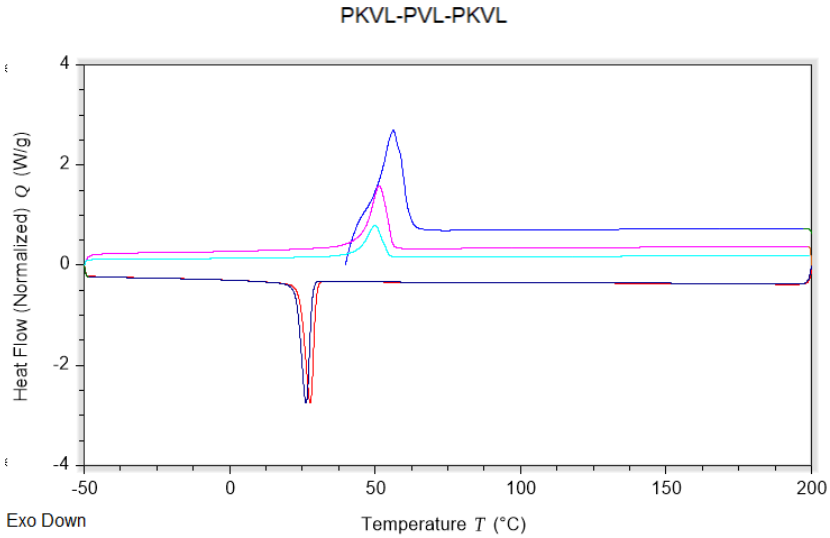

Figure 16. DSC thermogram for the 80:20 sample of **PKVL-PVL-PKVL**.

Biobased terephthalic acid from corn-derived products

Initial findings from the Dauenhauer group are described in the Figure 16, which outlines all three chemical steps to manufacture butadiene from corn-derived sugars. The initial green components include the decarbonylation reactor (R-1) followed by separating distillation columns D-1 and D-2; carbon monoxide and hydrogen are removed in a flash tank. In the purple reactor R-2, furan is then hydrogenated. In reactor R-3, tetrahydrofuran undergoes ring-opening dehydration to make butadiene; the energy is conserved via an economizing heat exchanger. Separations than occur in distillation columns D-3 and D-4 followed by drying in A-1.

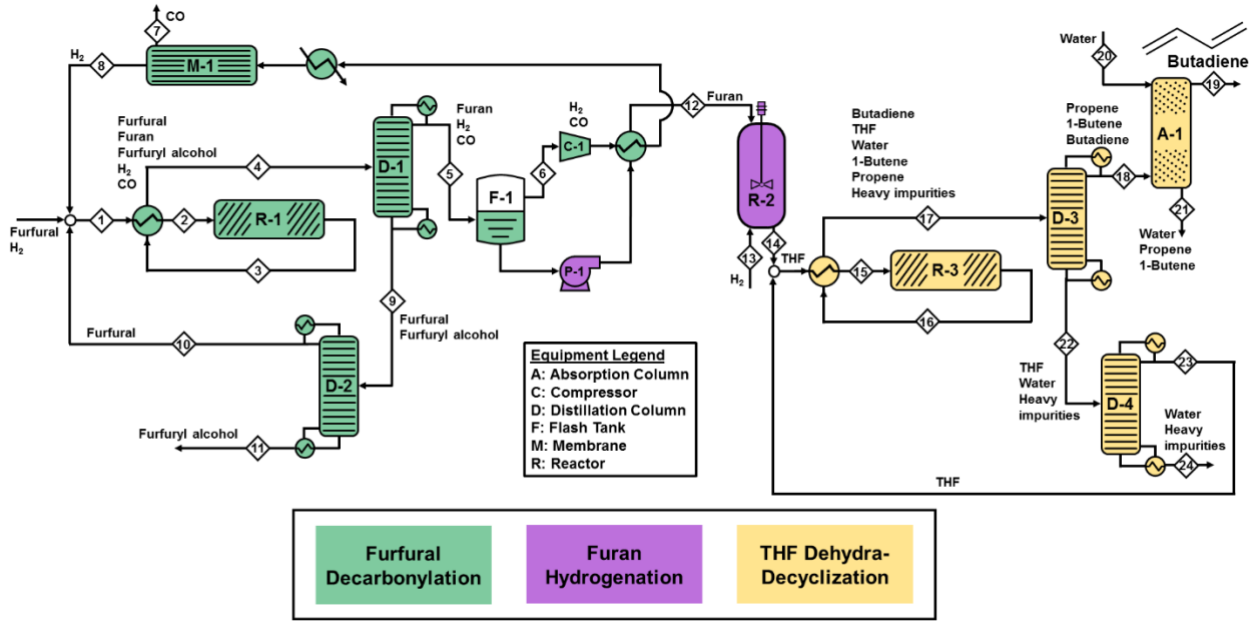

Figure 16

3.) CHALLENGES ENCOUNTERED. (*Describe any challenges that you encountered related to project progress specific to goals, objectives, and deliverables identified in the project workplan*.)

The Hillmyer group studied the replacement of mCPBA by greener oxidant. Unfortunately, the use of oxone led to no conversion in various conditions.

The Dauenhauer group determined that it is clear from the initial design that selective one-pass conversion in R-1 of furfural to THF would greatly improve the overall economics of renewable butadiene. However, this combined chemistry of decarbonylation and hydrogenation is not currently developed in a flow reactor system. This is a significant opportunity for research to have a direct impact on the economic improvement of sugar utilization. We will pursue and consider this option experimentally and via process simulation

4.) FINANCIAL INFORMATION (*Describe any budget challenges and provide specific reasons for deviations from the projected project spending*.)
Nothing to report.

5.) EDUCATION AND OUTREACH ACTIVITES. *(Describe any conferences, workshops, field days, etc attended, number of contacts at each event, and/or publications developed to disseminate project results.)*

Professor Jane Wissinger, with high school teachers Cassie Javner (Shakopee High School) and Cassie Knutson (White Bear Lake High School) hosted workshop for 19 high school teachers from across Minnesota from June 18-20, 2019. The workshop provided hands-on experience with laboratory experiments to integrate sustainable chemistry into high school curriculum. Some of the experiments introduced to teachers were developed by Professor Wissinger in the NSF Center for Sustainable Polymers. Participants completed post workshop evaluations indicating they had very positive experiences in the workshop, and that they intend to implement the experiments in their classrooms. Participating teachers do not incur any expenses for the participation, including all of their travel expenses and lodging at UMN during the workshop. This is thanks to the support from the MN Corn Research and Promotion Council and support from the UMN Materials Research Science and Engineering Center.

Workshop participants

References:

1. Cunha, M.; Fernandes, B.; Covas, J. A.; Vicente, A. A.; Hilliou, L., Film blowing of PHBV blends and PHBV-based multilayers for the production of biodegradable packages. J Appl Polym Sci 2016, 133 (2).
2. Tadmor, Z.; Gogos, C. G., Principles of polymer processing. John Wiley & Sons: 2013.
3. Geyer, R.; Jambeck, J. R.; Law, K. L., Production, use, and fate of all plastics ever made. Science Advances 2017, 3 (7), e1700782.
4. Schneiderman, D. K.; Hillmyer, M. A., 50th Anniversary Perspective: There Is a Great Future in Sustainable Polymers. Macromolecules 2017, 50 (10), 3733-3749.
5. Wooster, J.; Martin, J., Flexible Packaging Applications of Polyethylene. Handbook of Industrial Polyethylene and Technology 2018, 1071.
6. Mendez, J.; Annamalai, P. K.; Eichhorn, S. J.; Rusli, R.; Rowan, S. J.; Foster, E. J.; Weder, C., Bioinspired Mechanically Adaptive Polymer Nanocomposites with Water-Activated Shape-Memory Effect. Macromolecules 2011, 44 (17), 6827-6835.
7. Hsu, L.; Weder, C.; Rowan, S. J., Stimuli-responsive, mechanically-adaptive polymer nanocomposites. J Mater Chem 2011, 21 (9), 2812-2822.
8. Cudjoe, E.; Hunsen, M.; Xue, Z.; Way, A. E.; Barrios, E.; Olson, R. A.; Hore, M. J. A.; Rowan, S. J., Miscanthus Giganteus: A commercially viable sustainable source of cellulose nanocrystals. Carbohydrate Polymers 2017, 155, 230-241.
9. Habibi, Y.; Lucia, L. A.; Rojas, O. J., Cellulose Nanocrystals: Chemistry, Self-Assembly, and Applications. Chemical Reviews 2010, 110 (6), 3479-3500.

10. Okita, Y.; Saito, T.; Isogai, A., Entire Surface Oxidation of Various Cellulose Microfibrils by TEMPO-Mediated Oxidation. Biomacromolecules 2010, 11 (6), 1696-1700.
11. Isogai, A.; Saito, T.; Fukuzumi, H., TEMPO-oxidized cellulose nanofibers. Nanoscale 2011, 3 (1), 71-85.
12. Bucknall, C. B.; Karpodinis, A.; Zhang, X. C., A model for particle cavitation in rubber-toughened plastics. Journal of Materials Science 1994, 29 (13), 3377-3383.
13. Bucknall, C. B.; Paul, D. R., Notched impact behaviour of polymer blends: Part 2: Dependence of critical particle size on rubber particle volume fraction. Polymer 2013, 54 (1), 320-329.
14. Brown, H. R.; Argon, A. S.; Cohen, R. E.; Gebizlioglu, O. S.; Kramer, E. J., New mechanism for craze toughening of glassy polymers. *Macromolecules* **1989,** *22* (2), 1002-1004.
15. Gebizlioglu, O. S.; Beckham, H. W.; Argon, A. S.; Cohen, R. E.; Brown, H. R., A new mechanism of toughening glassy polymers. 1. Experimental procedures. *Macromolecules* **1990,** *23* (17), 3968-3974.
16. Allgaier, J.; Willbold, S.; Chang, T. *Macromolecules* **2007,** 40, (3), 518-525.
17. Pangborn, A. B.; Giardello, M. A.; Grubbs, R. H.; Rosen, R. K.; Timmers, F. J., Safe and Convenient Procedure for Solvent Purification. *Organometallics* **1996,** *15* (5), 1518-1520.